

Contract No:

This document was prepared in conjunction with work accomplished under Contract No. DE-AC09-08SR22470 with the U.S. Department of Energy (DOE) Office of Environmental Management (EM).

Disclaimer:

This work was prepared under an agreement with and funded by the U.S. Government. Neither the U. S. Government or its employees, nor any of its contractors, subcontractors or their employees, makes any express or implied:

- 1) warranty or assumes any legal liability for the accuracy, completeness, or for the use or results of such use of any information, product, or process disclosed; or
- 2) representation that such use or results of such use would not infringe privately owned rights; or
- 3) endorsement or recommendation of any specifically identified commercial product, process, or service.

Any views and opinions of authors expressed in this work do not necessarily state or reflect those of the United States Government, or its contractors, or subcontractors.

(Oxy)hydroxides Formed on Aluminum Fuel Materials After Irradiation and Long-Term Wet Storage – 20354

Anna L. d'Entremont*, Luke C. Olson**, Christopher G. Verst*, Roderick E. Fuentes*,
Robert L. Sindelar*

*Savannah River National Laboratory, Aiken, SC

**Westinghouse Electric Company, Columbia, SC

ABSTRACT

The aluminum cladding of research-reactor fuel experiences general corrosion when in contact with water during in-reactor service and post-discharge wet storage, resulting in the formation of adherent aluminum (oxy)hydroxide films. These (oxy)hydroxides contain chemically-bound water that poses challenges for extended dry storage due to the risk of thermal or radiolytic decomposition releasing free water and/or hydrogen and oxygen gases. This study describes characterization of the (oxy)hydroxides present on several aluminum materials used in reactor operation and subsequently stored wet in the L-Basin storage facility at the Savannah River Site (SRS) for an extended period. Characterization data providing insight into the loading, composition, and morphology of (oxy)hydroxides to be expected on service-exposed aluminum cladding provides valuable benchmarks for designing adequate drying and dry-storage approaches.

This work is part of a broader investigation to address knowledge gaps and technical data needs for dry storage of aluminum-clad spent nuclear fuel (ASNF), which included in-lab growth of (oxy)hydroxide films on aluminum alloy substrates to investigate formation behavior, investigation of drying methods to remove existing (oxy)hydroxides from ASNF cladding, and measurement of radiolytic yield of hydrogen from (oxy)hydroxide powders and films.

In this study, (oxy)hydroxide films were characterized for three aluminum-alloy materials used in reactors and subsequently stored wet for up to approximately 40 years in L-Basin at SRS: one cropping from a Missouri University Research Reactor (MURR) fuel element (Al-6061 alloy), one cropping from a Universal Sleeve Housing (USH) (Al-6063 alloy), and one Mark-16B fuel assembly (either Al-6061 or Al-6063). The USH and Mark-16B were used in SRS production reactors. Characterization of the as-received (oxy)hydroxides included scanning electron microscopy (SEM) in both plan-view and cross-section to characterize the (oxy)hydroxide layer's morphology, thickness, and structure. X-ray diffraction (XRD) was used to identify the chemical composition and distinguish between the various aluminum (oxy)hydroxides known to form under reactor and storage conditions.

XRD analysis revealed both bayerite ($\text{Al}(\text{OH})_3$) and boehmite (AlOOH) on the surface of the MURR and USH samples, as well as bayerite, boehmite, and gibbsite (another $\text{Al}(\text{OH})_3$ polymorph) on the surface of the Mark-16B sample. The aluminum trihydroxides, bayerite and gibbsite, are typically associated with corrosion in low-temperature ($<80^\circ\text{C}$) water, while boehmite is expected to form at higher water temperature ($>80^\circ\text{C}$). The presence of bayerite on the USH, which is believed to have operated close to 90°C , suggests that boehmite formed during in-reactor exposure was not protective against further hydroxide growth in low-temperature wet storage.

Cross-section scanning electron microscopy (SEM) showed total (oxy)hydroxide layer thicknesses of ~ 5 – $10\ \mu\text{m}$ for the MURR and ~ 5 – $15\ \mu\text{m}$ for the Mark-16B. The thickness of the USH's (oxy)hydroxide layer was indiscernible by the current mounting and imaging method, despite plan-view SEM and XRD confirming the presence of an (oxy)hydroxide layer.

INTRODUCTION

Motivation for Sampling (Oxy)hydroxides on L-Basin Fuel Croppings

Characterizing the structure and composition of the aluminum (oxy)hydroxides observed on actual Aluminum-Clad Spent Nuclear Fuel (ASNF) cladding is important to inform tasks associated with ASNF disposal. During dry storage of ASNF, (oxy)hydroxides on the cladding are a potential source of hydrogen through radiolysis or water through desorption or thermal decomposition, both of which may be dependent on the morphology and composition of the (oxy)hydroxide film. The present sampling of actual ASNF aims to identify and characterize the oxyhydroxides present on ASNF cladding.

Material Storage Histories and Retrieval from L-Basin

Fig. 1 shows the cropping pieces in their respective storage bins in L-Basin prior to retrieval for shipment to SRNL. One cropping each from a MURR fuel element, a universal sleeve housing (USH), and a Mark-16B assembly were collected underwater in the basin (Fig. 2, left), transferred underwater to a shipping cask, and shipped to SRNL in late August 2018. Pieces were drip-dried in the SRNL shielded cells facility.



Fig. 2. Scrap and croppings in wet storage in L-Basin.

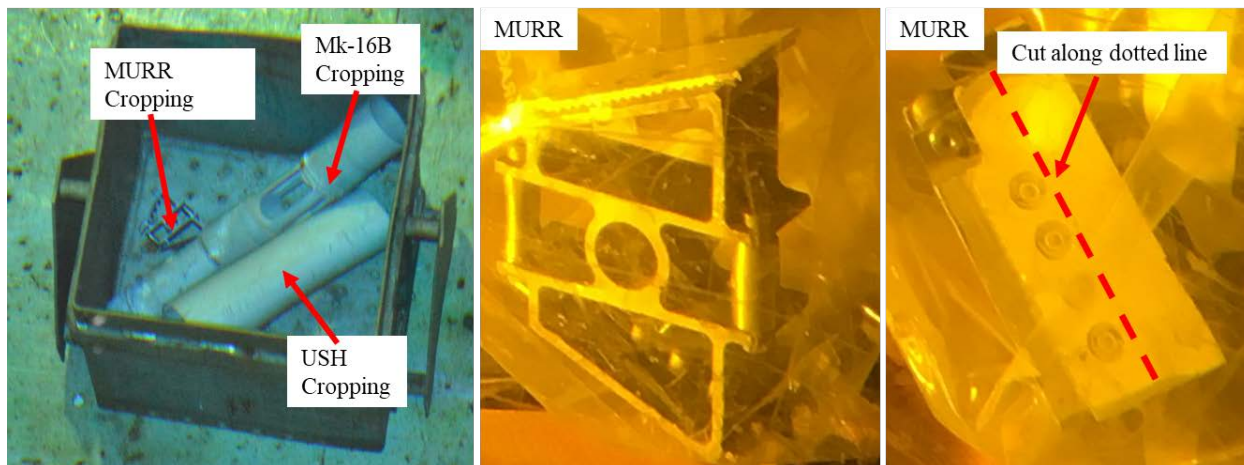


Fig. 1. (Left) L-Basin croppings to be analyzed; (middle and right) MURR piece in shielded cells.

MURR Cropping

The entire structure of the MURR fuel element was fabricated of aluminum alloy 6061-T6 with stainless steel hardware.[1] The MURR has a well-documented history of in-reactor and storage conditions. However, the MURR cropping sampling was retrieved from a bucket of multiple croppings (Fig. 1, middle), and thus fuel-element-specific information was lost, including what element it was cropped from and whether the cropping was from the top or bottom of the element. This complicates determining a thermal history for the MURR sample. A minimum in-core temperature range, while operating under full power,

can be estimated using operating parameters and core design knowledge. Note that passivation film growth during non-operation times is unknown. In the MURR core design [2], nearly all the coolant water flows past the plate fuel in the elements. Based on core coolant average entry temperature of 60°C and average exit temperature of 70.7°C [1], it can be estimated that the piece evaluated was at least 60°C if from the inlet end of the element or near 70.7°C if from the exit end. The temperatures could have been higher than 70.7°C because the fuel elements generated power along their length and were in direct contact with the slotted aluminum side plate sampled. However, the high fuel-plate surface area and rapid drop off in power level as a function of distance from the center of the core could lessen this effect.[3]

As of 2013, over 35 years of operation, the MURR averaged 6.3 days of operation each week and discharged fuel elements after about 18–20 weeks of in-core operation.[3] Each element therefore operated in-core about 113–126 days at temperature. The 18–20 weeks of operation were non-sequential: all fuel elements were removed from the core every week and replaced with other elements that were either fresh or stored from previous runs, so that the core could start xenon-free each time.[3]

A minimum temperature of 60°C and a minimum time at temperature of 113 days can be assumed bounding for the MURR sample. After each ~6.3 days of operation, the fuel spent no less than 7 days in wet storage. When outside the core, the fuel was stored in the main pool with a mixed bulk temperature of 37.8°C.[1] In 2018, the maximum pool pH was 6.45; the minimum was 5.18, and the average was 5.77.[4] In 2018, the maximum pool conductivity was 2.72 mS/m; the minimum was 0.95 mS/m, and the average was 1.49 mS/m.[4] Other years are assumed to be similar. After final discharge from the reactor, the fuel was shipped to SRS L-Basin where it was put in a storage pool and cropped. The MURR cropping arrived in L-Basin no earlier than 2000, since offsite fuel was previously sent to the Receiving Basin for Offsite Fuel, and croppings were not moved from that facility when it was de-inventoried of used/spent fuel.

Due to the low power of the MURR (5–10 MW) [1] and estimated cladding temperature of around 60°C – 70°C during operation, this fuel is expected to have a thin (oxy)hydroxide layer composed primarily of aluminum trihydroxide (gibbsite and/or bayerite). Boehmite could also be present if the temperature was high enough due to, e.g., proximity to the fuel meat dissipating heat.

USH Cropping

USHs were made from aluminum alloy 6063 and used in the heavy-water production L-Reactor operated at SRS.[5, 6] While the USHs were not deliberately pretreated to form a protective boehmite surface prior to operation, they did undergo flow testing including steam drying, which likely formed some boehmite on the surface. The steam drying used superheated steam and lasted about 5–10 minutes, although the exact superheated steam temperatures and times used could not be determined.[7] The USH cropping average exposure temperature was estimated from the process water system heat exchanger design data, obtained from Table 5.4-1 in the SRS Production Reactor Safety Analysis Report (SAR).[8] The process water heat exchanger had an average inlet temperature of 37.8°C and an average outlet temperature of 93.3°C.[8] The exact location of the USH cropping in relation to its placement in the core is unknown, so its temperature history could fall anywhere in this range. However, the USH croppings remaining in L-Basin are believed to be primarily from the active fuel length, which is expected to be closer to the core outlet than inlet temperature. The USHs were in core for about 5 years prior to replacement [9], after which they were stored wet in L-Basin since the 1970s.

Mark-16B Cropping

The Mark-16B cropping is from either the P, K, or L heavy-water production reactor.[6] SRS drawings indicate the Mark-16B cropping was from the “auxiliary sleeve”, and could have been fabricated using either Al-6061 (tempers T4, T6, T651, or T6511) or Al-6063 (tempers T4, T6, T651, or T6511).[10] Mark-

16B assemblies were not deliberately pretreated to form a protective boehmite surface prior to operation, but did undergo flow testing including steam drying similar to that performed on the USH, which likely formed some boehmite on the surface.[7] Indentations on the cropping and visible in SRS drawings indicate the cropping came from the top of the assembly[11]. SRS production reactor coolant flowed from the top down, so the Mark-16B cropping probably saw temperatures close to the inlet temperature of 37.8°C. The Mark-16B assemblies were kept in core for ~7 months [9], after which they were stored wet since the 1970s.

L-Basin Storage Conditions

The impact of corrosion during wet storage should also be considered. L-Basin temperature and chemistry have been actively monitored throughout its history. During the 1970s and early 1980s, water conductivity was maintained in the 60–70 $\mu\text{S}/\text{cm}$ range.[12] Changes in pool chemistry associated with L-reactor mothballing and shutdown led to higher conductivity conditions, with conductivity ranging between 90 and 120 $\mu\text{S}/\text{cm}$ during the 1987–1991 period and a peak in 1991 reaching ~160 $\mu\text{S}/\text{cm}$. [12] The higher conductivity during this period was largely attributable to storage conditions where dissimilar metals were in contact, leading to galvanic corrosion. These conditions have since been remedied. Extensive deionization began in L-Basin in early 1994, and a series of deionizer systems were tested, bringing the conductivity down to near current values.[12] L-Basin chemistry has been recorded since ~12/1992, with temperature available since ~10/1996. TABLE I summarizes the L-Basin storage pool chemistry data from 12/1992–12/2018.

TABLE I. L-Basin storage pool temperature and chemistry 12/1992–12/2018.

| | | 12/1992–12/2018 | |
|---|---------|------------------------|------------------------|
| pH | Maximum | 8.0 | |
| | Minimum | 5.1 | |
| | Average | 6.5 | |
| | | 12/1992–12/1995 | 01/1996–12/2018 |
| Conductivity ($\mu\text{S}/\text{cm}$) | Maximum | 159.0 | 7.8 |
| | Minimum | 2.40 | 0.02 |
| | Average | 97.7 | 1.3 |
| | | 10/1996–12/2018 | |
| Temperature (°C) | Maximum | 28.0 | |
| | Minimum | 14.6 | |
| | Average | 22.3 | |

TABLE II summarizes the croppings' estimated minimum temperature and durations of the operation and storage phases of the samples' histories, based on review of documentation on the reactors and storage basins.

TABLE II. Estimated cropping in-reactor operation and post-discharge basin storage history.

| Cropping | Minimum Operation Temperature (°C) | Operation Time (days) | Storage Temperature (°C) | Storage Time (years) |
|-----------------|---|------------------------------|---------------------------------|-----------------------------|
| MURR | 60 | 113 | 22.3 ^b | <18 |
| USH | 37.8 ^a | ~1800 | 22.3 ^b | ~40 |
| Mark-16B | 37.8 | ~220 | 22.3 ^b | ~40 |

^aThe cropping is likely from an active fuel region and therefore its temperature may have been as high as the maximum outlet temperature of 93.3°C.

^bAverage L-Basin temperature from 12/1992–12/2018.

Literature Models for (Oxy)hydroxide Growth

A literature search was performed for available data and correlations to estimate (oxy)hydroxide layer thickness based on the croppings' service histories to provide a rough comparison between current observations and those in the literature and was described in more detail in Ref. [13]. Estimates based on the literature correlations considered only in-core exposure, ignoring potential growth during wet storage due to lack of data and correlations for (oxy)hydroxide growth over a pre-existing (oxy)hydroxide film. It is assumed that the (oxy)hydroxides were predominantly formed in-core rather than in storage due to the higher temperatures and the fact that higher-temperature (oxy)hydroxides are generally more protective.

Several studies reported the metal loss per area L (mg/dm²) rather than (oxy)hydroxide mass or thickness. The metal loss L can be converted to oxide thickness x_{ox} , assuming a dense and completely adherent film, by

$$x_{ox} = \frac{L}{M_{Al}} \frac{M_{ox}}{\rho_{ox}} \quad (\text{Eq. 1})$$

where $M_{Al} = 27$ g/mol and M_{ox} are the molar masses of Al metal and the (oxy)hydroxide, respectively, and ρ_{ox} is the (oxy)hydroxide density. For either trihydroxide, $\text{Al}(\text{OH})_3$, the molar mass is $M_{ox} = 78$ g/mol. The trihydroxide densities differ slightly: $\rho_{ox} = 2.42$ g/cm³ for gibbsite and $\rho_{ox} = 2.53$ g/cm³ for bayerite.[14] For boehmite, the expected oxide above 80°C, the molar mass is $M_{ox} = 60$ g/mol and the density is $\rho_{ox} = 3.01$ g/cm³. [14] Note that the actual film could be porous, tending to increase the thickness for a given amount of corrosion, or could be a mixture of two or more (oxy)hydroxides.

For MURR, the closest data found was corrosion of Al-1100 in 70°C, 6.5 pH, oxygen-saturated water for up to 1.5 years [15]. The areal mass of metal lost L was fitted with a logarithmic expression with two fitting parameters whose values differed based on whether the corrosion was in fresh water or water from another corrosion test vessel bearing corrosion products [15]. For MURR, the cumulative exposure time was estimated to be 113–126 days in-core and 239–266 days total service life (alternating operation and wet storage). The Ref. [15] correlation predicts x_{ox} of 4–5 μm for 113–266 days of exposure [13]. Note that the MURR cropping would have been exposed to forced coolant flow, while the Draley correlations were derived for minimal-flow conditions, and the impact of water velocity on the oxide formation is uncertain.

For USH, two comparisons were found, assuming it was exposed to near-outlet temperatures $\sim 93^\circ\text{C}$. However, neither was derived from data for Al-6063, and both correlations have been extrapolated far beyond the duration of the original data. Draley et al. [16] measured corrosion of Al-1100 at 95°C for O_2 -saturated and He-saturated water for up to 45 days. The areal metal loss L was fitted with a logarithmic expression with two fitting parameters. For USH with 5 years (1825 days) in-core exposure, the Ref. [16] correlation predicts an (oxy)hydroxide thickness of ~ 2 μm . As for MURR, the USH would have been exposed to forced coolant flow rather than the minimal flow of the Ref. [16] tests. Pawel et al. [17] measured corrosion of Al-6061 in a test loop with forced water flow at 9–28 m/s, 4.5–5.0 pH, heat flux of 5–20 MW/m², calculated water-oxide interface temperatures of 95–208°C, and durations up to 35 days. The (oxy)hydroxide layer thickness was fitted as a power law with exponent 0.74 and rate constant depending on the initial oxide thickness, water-oxide interface temperature, and heat flux [17]. For USH, with 5 years (43800 hours) exposure at about 90°C assuming no pre-existing film and negligible heat flux, Ref. [17] correlation predicts a thickness of 16 μm .

For Mark-16B, the closest data found was in-reactor corrosion testing by Neumann [18, 19] on aluminum coupons of multiple alloys in the Oak Ridge Research Reactor (ORR), which operated in cycles of 3 weeks operation followed by ~ 1 week downtime. Corrosion specimens were removed after various numbers of cycles. The water flowrate was estimated to be 8–12 ft/s; the core inlet and outlet temperatures were 124°F (51°C) and 132°F (56°C), respectively, at power (somewhat higher than the estimated $\sim 38^\circ\text{C}$ operating temperature for the Mark-16B), and the pH was usually in the range 5.5–6.5 [19]. The measurement of

metal loss was complicated by incomplete defilming in some cases, for unknown reasons [18, 19]. After 3 weeks at power, the measured mass losses of 0–1.0 mg/cm² [18] would correspond to 0–12 µm of dense trihydroxide. After 24 weeks exposure (~14 weeks at power), the measured weight loss of 0–1.2 mg/cm² [18] would correspond to 0–14 µm of dense trihydroxide. Due to the small increase from 3 to 24 weeks, the 24-week range of 0–14 µm is taken as the closest comparison to the Mark-16B's estimated 7 months (about 32 weeks) of in-core exposure.

DESCRIPTION

Methods

Sample Preparation

At SRNL, the MURR piece was removed from the water in the cask and placed in a closed Ziploc® bag in the shielded cells until the stainless steel bolts were cut off using a Dremel®. It was then double-bagged and taped shut for transport out of the shielded cells. Removing the bolts reduced the dose associated with the cropping and allowed for its transfer out of the shielded cells and into a radiological hood. In the radiological hood, an attempt at further decontamination was made by scrubbing the cropping with a soft bristle brush prior to cutting samples using a slow-speed abrasive saw.

The MURR cropping, with the section removed for characterization (SEM) marked, is shown in Fig. 2., middle and right. The cropping was cut along the red dotted line shown in Fig. 2. (right) using a slow speed abrasive saw. The section removed was further cut into 4 samples using the same method. One sample was characterized by x-ray diffraction (XRD), one by plan-view scanning electron microscopy (SEM) and energy dispersive spectroscopy (EDS), one was cross-sectioned and mounted for SEM and EDS, and one was retained as a spare. The surface that faced the inside of the fuel element, with a slotted edge, was the face examined by XRD and plan-view SEM/EDS. The inside surface was chosen due to disturbance of the other surfaces by the decontamination attempt (the brush used could not reach the inside surface).

Once at SRNL, the Mark-16b and USH croppings were removed from the cask and allowed to drip dry for several hours before being double bagged, J-sealed, and stored until samples were cut and sent for analysis. Fig.3 shows the regions of the USH (left) and Mark-16B (right) croppings where the samples were cut for analysis. For USH, straight-cut aviation snips were used to cut a roughly square piece from the edge and divide it into smaller pieces according to the grid shown in Fig.3 (left). For Mark-16B, large bolt cutters were used to cut five pieces from the water inlet as marked in Fig.3 (right). Samples 1–4 for each material were dispositioned like the MURR pieces; the fifth Mark-16B sample was also kept as a spare.

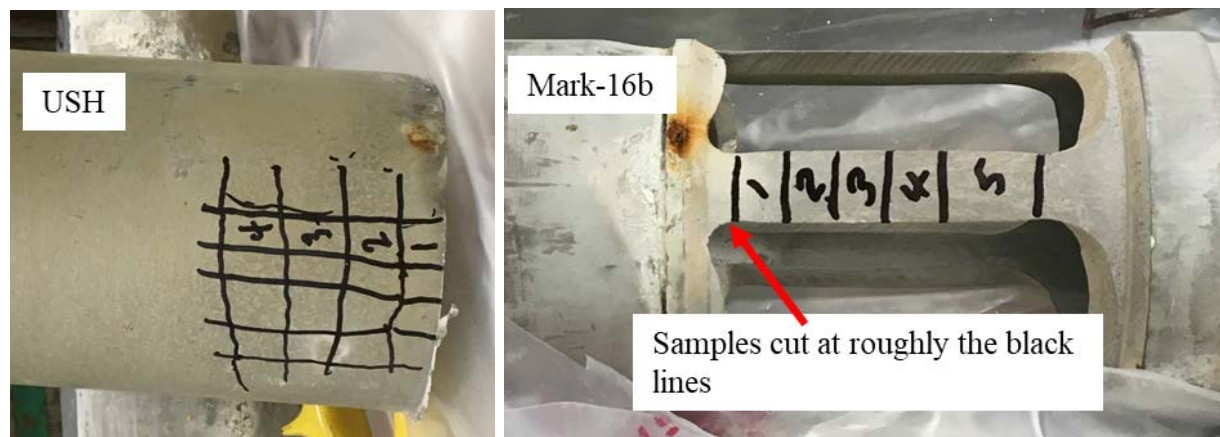


Fig.3 (Left) USH cropping and (right) Mark-16B cropping marked for cutting of samples.

Samples used for cross-section SEM/EDS were mounted together in EpoFix. Glass slides were placed between samples in the epoxy mount to reduce pressure on the samples during grinding and polishing.

The EDS results should be interpreted with caution. In general, EDS spatial resolution can be expected to range from a micron to several microns in diameter on the sample surface and into the sample.[20] The spatial resolution of a particular measurement is a function of the sample chemistry, density, and the SEM accelerating beam voltage.[21] The Anderson and Hasler model [21] for x-ray generation range predicts the spatial resolution for Al and O as about $3.6\text{ }\mu\text{m}$ in a material with a density of 2.7 g/cm^3 (aluminum) and about $2.5\text{ }\mu\text{m}$ in a material with a density of 4 g/cm^3 (e.g, Al_2O_3). The densities and thus spatial resolutions for the aluminum (oxy)hydroxides fall between these bounds.

Results

XRD Analysis

The XRD spectra for the MURR, USH, and Mark-16B croppings are shown in Fig.4, Fig.5, and Fig.6, respectively. Comparison of the XRD spectra show that the (oxy)hydroxide peaks become stronger in relation to the base aluminum peaks from the MURR to the USH and finally the Mark-16B, implying progressively thicker (oxy)hydroxide layers. Similar visual observations were made during sample cutting. Bayerite and boehmite were found on all three samples, but gibbsite was found on only the Mark-16B, believed to have operated in the coldest environment. The intensity of the boehmite peaks relative to the bayerite peaks was largest for the USH, while the (oxy)hydroxide peaks in the Mark-16B appeared to be dominated by the trihydroxides (scale-adjusted XRD plots can be seen in Ref. [13]).

Planview SEM

Fig.7 and Fig.8 show planview SEM of the MURR and USH, respectively. Their (oxy)hydroxides appear to have remained intact from wet storage and unaffected by decontamination attempts on the MURR. Both appear to be blocky and dense, similar to that observed on a dry-stored RU-1 fuel plate [22] and similar to

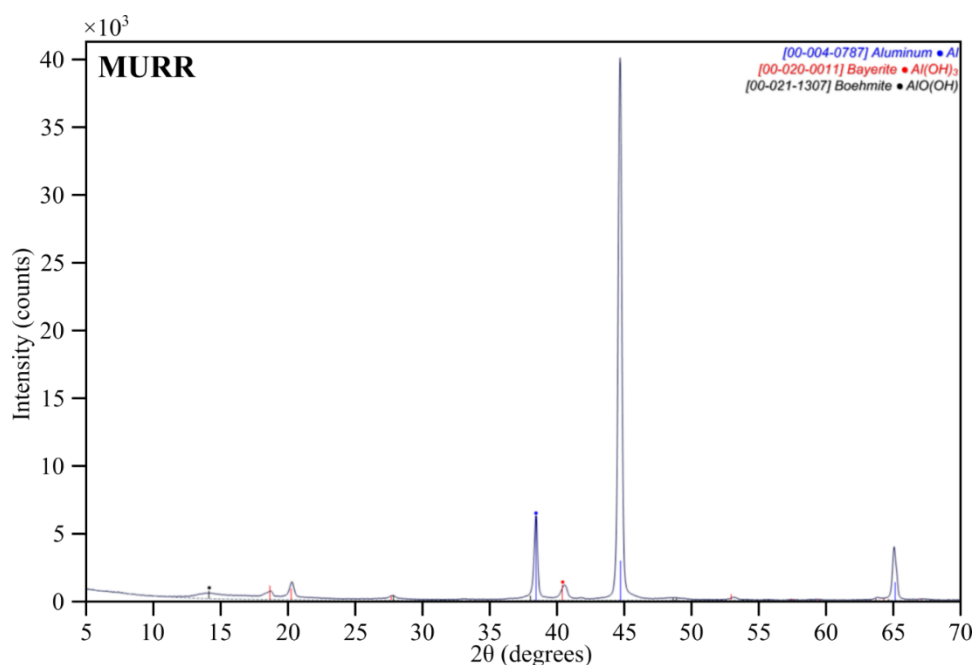


Fig.4 XRD spectrum of MURR sample, displaying bayerite and boehmite peaks.

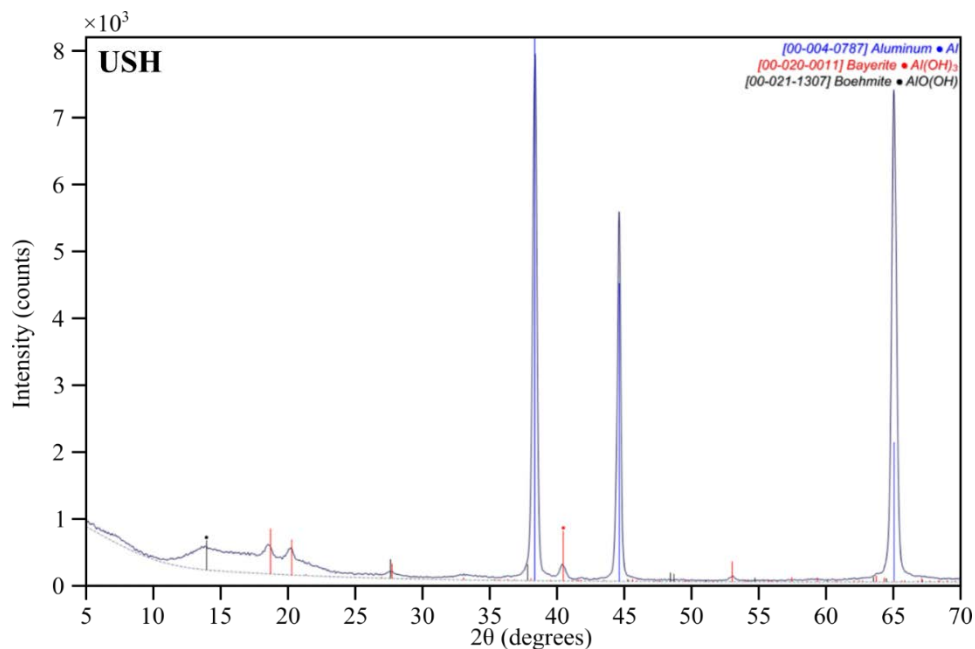


Fig.6 XRD spectrum of USH cropping oxide, displaying bayerite and boehmite peaks.

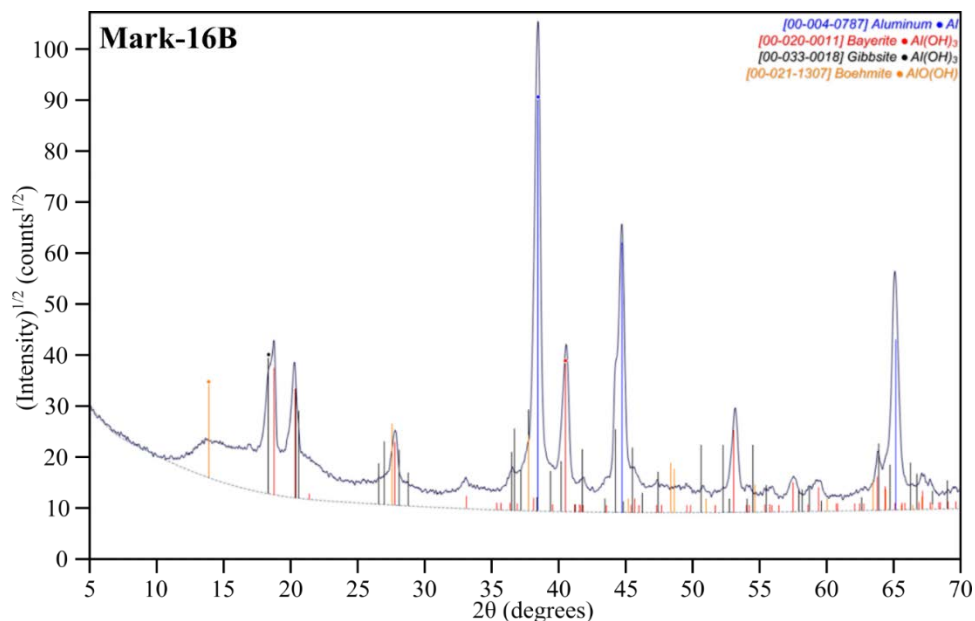


Fig.6 XRD spectrum of Mark-16B cropping oxide, displaying bayerite, gibbsite, and boehmite peaks.

lab-grown bayerite films grown at low temperature for durations greater than about a month [23]. The (oxy)hydroxide on the USH appears to be denser and smoother than on the MURR sample.

The (oxy)hydroxide film on the Mark-16B sample was found to have spalled off near an edge (Fig.9), which was assumed to be caused by the cutting operation utilizing a bolt-cutter. This provided an opportunity to examine both the thick (oxy)hydroxide film and the surface beneath it. EDS results (presented below) suggest a thinner oxide remains in this region.

Fig.10 (top) shows the thick (oxy)hydroxide. It appears to be blocky in morphology, with a highly irregular surface resulting in a porous structure. Fig.10 (bottom) shows the spalled oxide region. The (oxy)hydroxide

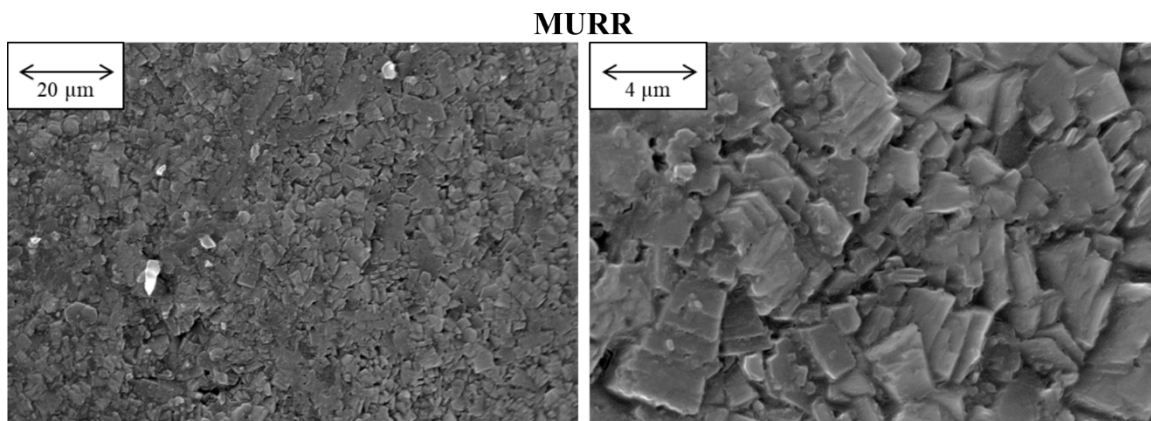


Fig.9 SEM Plan-view of MURR oxide

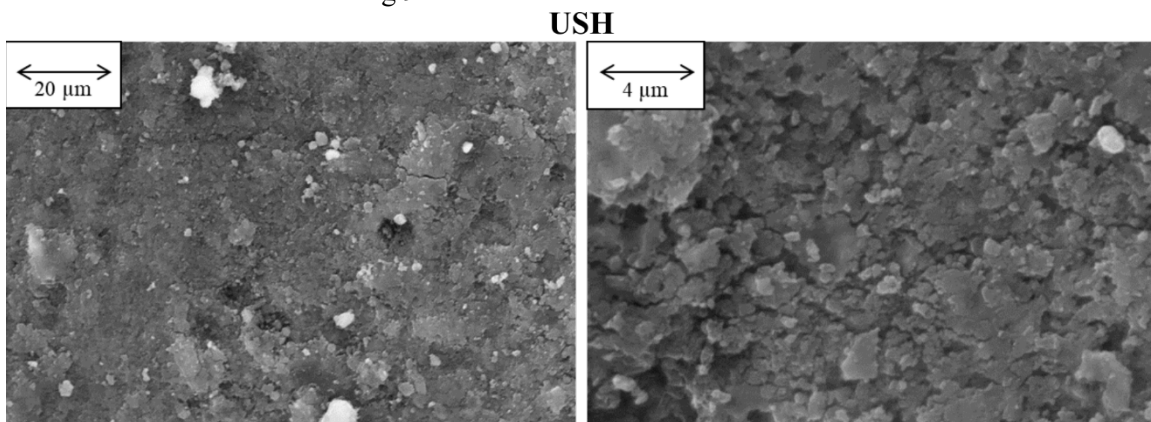


Fig.9 SEM plan-view of the surface of a USH cropping

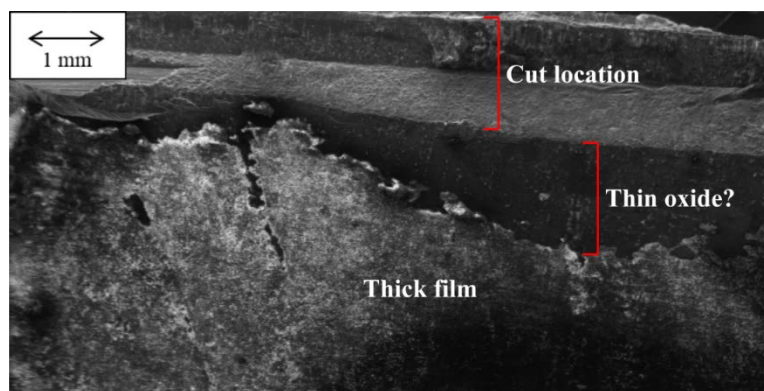


Fig.7 Top: SEM showing region of Mark-16B sample near cut edge with broken oxide.

appears to be nodule-like. Sporadic pits are visible, but the film appears overall more uniform and denser than the thick film.

Cross-section SEM and EDS

Fig. 11 shows the cross-section SEM for the (left) MURR, (center) USH, and (right) Mark-16B (oxy)hydroxide films. Each image is oriented so that the mounting material, which appears black, is on the

left side of the image, and the aluminum alloy substrate (light gray) is on the right side. The EDS line-scan locations are marked in red on each cross-section.

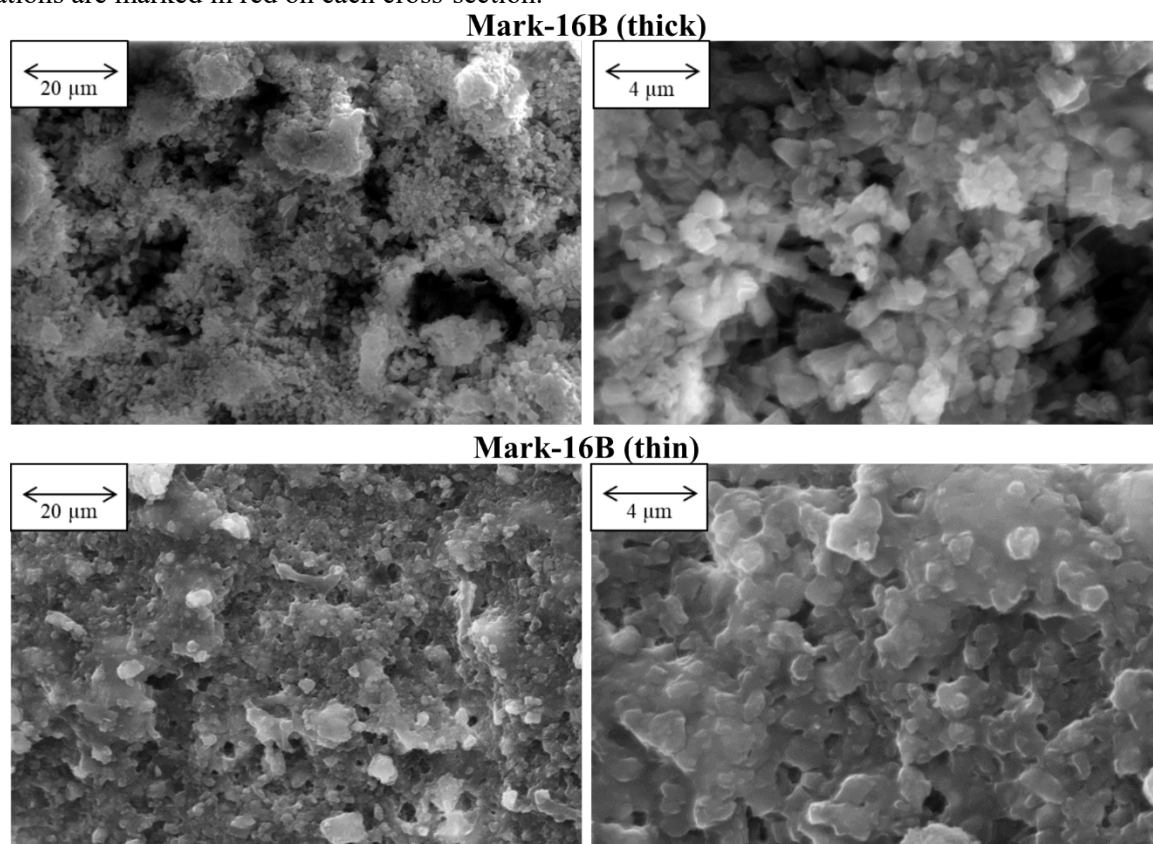


Fig.11 Planview SEM of the surface of the Mark-16B sample, showing both the thick and thin regions.

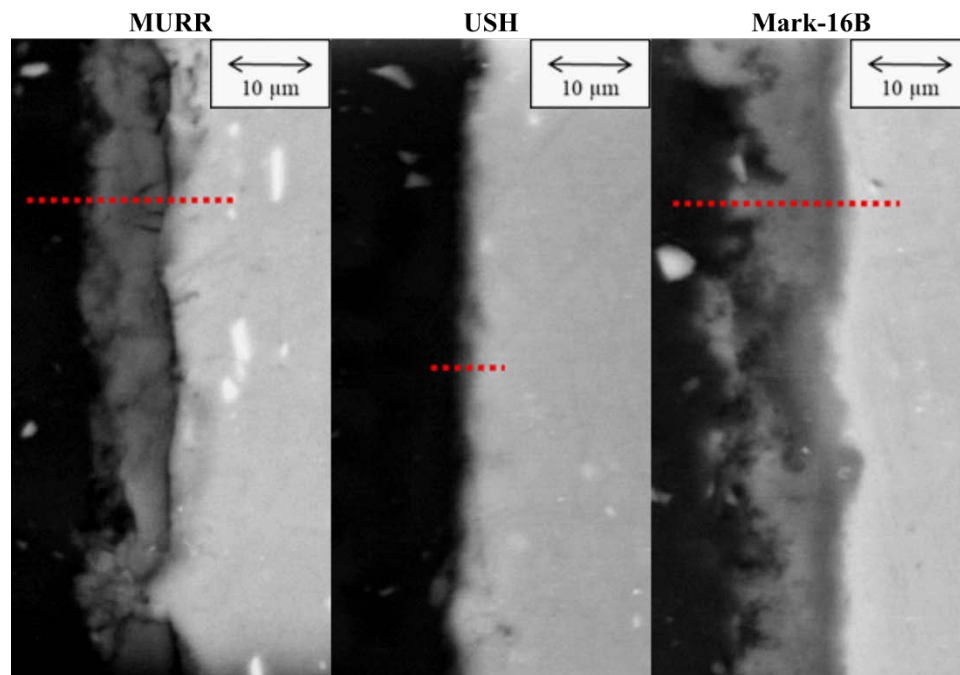


Fig. 10. Cross-section SEM of (oxy)hydroxide layers on the (left) MURR, (center) USH, and (right) Mark-16B samples with EDS line scan locations marked with red dashed lines.

The (oxy)hydroxide layer on the inside stepped edge of the MURR sample Fig. 11 (left), which would have been between the grooves holding the fuel plates, was $\sim 5\text{--}10\ \mu\text{m}$ thick. It was relatively uniform in thickness over the region examined, staying mostly $\sim 10\ \mu\text{m}$ in thickness. The MURR EDS line-scan results are shown in Fig. 12(top). It shows an oxygen-enriched passivation layer in the $\sim 8\text{--}16\ \mu\text{m}$ beam position range, and a gradual increase in the aluminum concentration from left to right as the EDS measurements are taken progressively closer to the metal substrate. The carbon from the mount as well as from contamination influences the relative amount of aluminum and oxygen detected, so the ratio of oxygen to aluminum may not be a reliable metric to determine the oxide polymorph.

The USH sample cross-section is shown in Fig. 11 (center) and the EDS line-scan in Fig. 12 (middle). The SEM and EDS cross-section results did not reveal a discernible oxide. The lack of discernible oxide suggests that it was either a very thin layer or did not survive the sample preparation process. Given that

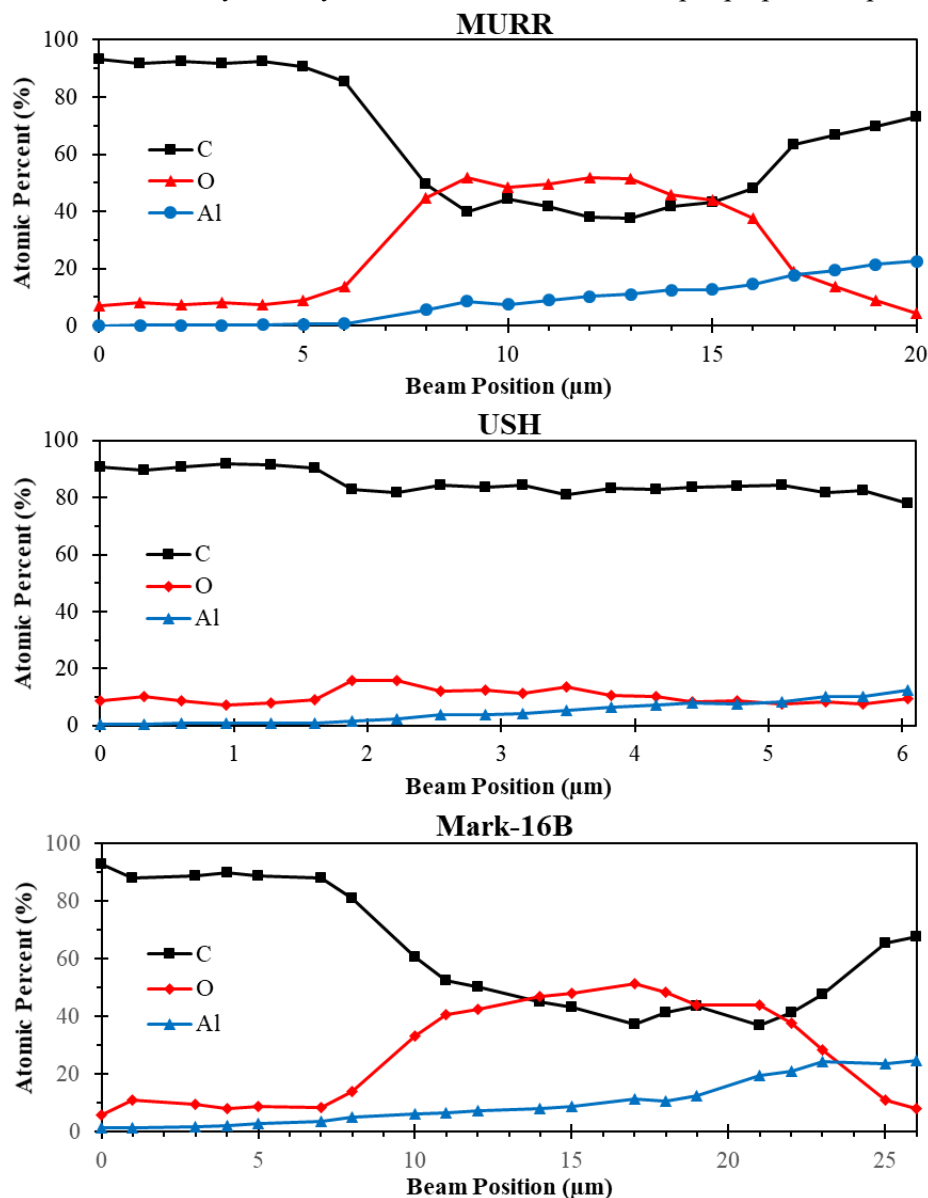


Fig. 12. EDS line scan for (top) MURR, (middle) USH, and (bottom) Mark-16B samples corresponding to the dashed red lines in Fig. 11. EDS results have been normalized to show exclusively carbon (present in the mounting material and as surface contamination), aluminum, and oxygen.

the (oxy)hydroxide layers survived the sample preparation on the MURR and Mark-16B, an (oxy)hydroxide being visible in the USH plan-view SEM, and XRD indicating that the USH film was mostly boehmite (an oxide that develops slowly), it is believed that the (oxy)hydroxide is present but very thin ($<1\ \mu\text{m}$). It is possible that a technique providing better contrast and edge retention, such as Ni plating, may allow for imaging of the thin (oxy)hydroxide layer, if present. The EDS line scan in Fig. 12(middle) does show a small bump in oxygen content that may reflect the presence of a thin oxide layer. There is also a gradual increase in the aluminum concentration from left to right as the EDS measurements are taken progressively closer to the metal substrate.

The Mark-16B thick oxide sample cross-section is shown in Fig. 11 (right), with EDS line-scan in Fig. 12 (bottom). The oxide was relatively uniform over the surface cross-section examined and varied from ~ 5 to $\sim 15\ \mu\text{m}$ in thickness, but on average appeared to be about $10\ \mu\text{m}$. The EDS line scan in Fig. 12(bottom) shows the oxide enriched passivation layer and a gradual increase in the aluminum concentration from left to right as the EDS measurements are taken progressively closer to the metal substrate.

Plan-View EDS

EDS of the plan-view oxides was performed to verify the presence of oxide and obtain an additional indication of thickness. Fig.13 shows the oxide surfaces with the region of the EDS raster scans marked. The EDS results are summarized in TABLE III. For thin oxide films, the active region contributing to the EDS signal could extend through the oxide and into the aluminum base alloys so that the results do not solely reflect oxide composition, as previously mentioned. Based on the complete aluminum (oxy)hydroxide chemical formulas, the atomic percent of oxygen should be 50% for pure, thick boehmite (AlOOH), 43% for gibbsite and bayerite ($\text{Al}(\text{OH})_3$), and 60% for alumina (Al_2O_3). However, EDS cannot detect hydrogen, so atomic percentages measured by EDS are expected to be 67% O for boehmite and 75%

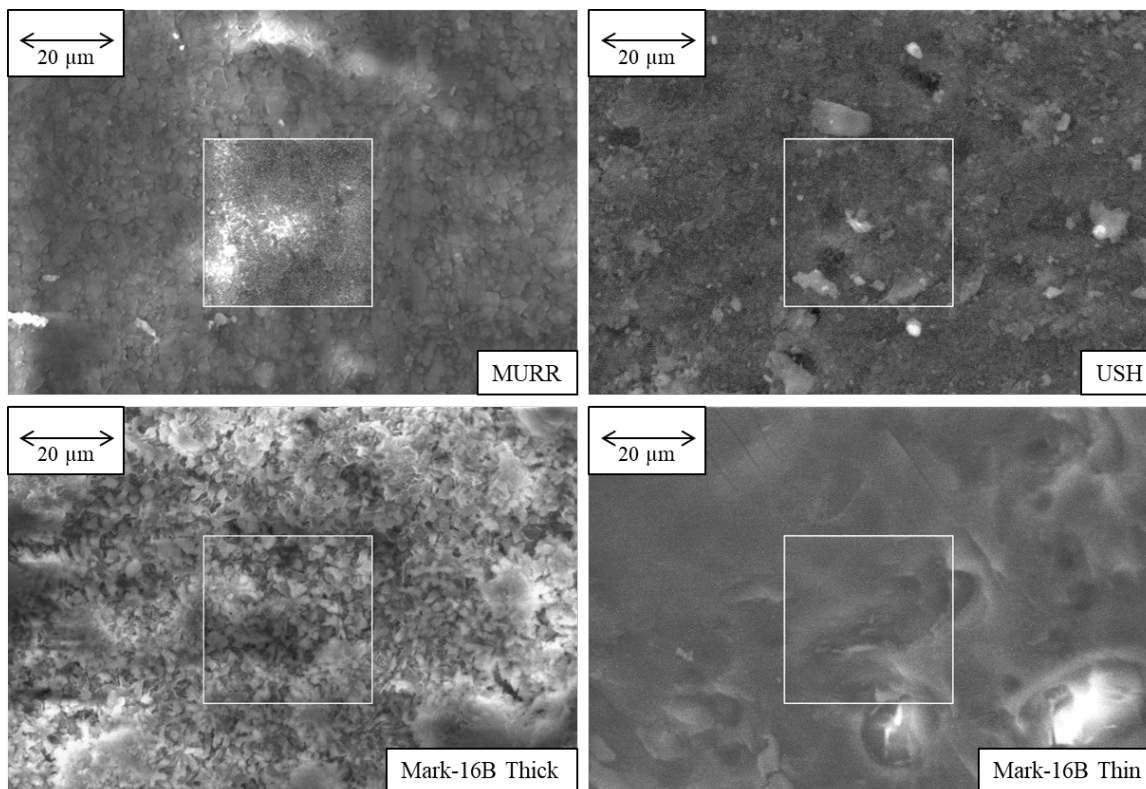


Fig.13 SEM with boxes marking the regions of the EDS area scan.

O for gibbsite and bayerite. Note that alumina forms in air at room temperature but is not stable in water until temperatures exceed 360°C.[14]

TABLE III EDS area scan data corresponding to regions in Fig.13.

| | All results | | | | | | | Results for O and Al only (data renormalized) | |
|-------------------|-------------|-----|------|-----|-----|-----|-----|--|------|
| | (atomic %) | | | | | | | (atomic %) | |
| Sample | O | Mg | Al | Si | S | Fe | Zn | O | Al |
| Thick oxide Mk16B | 79.8 | | 20.1 | 0.2 | | 0.0 | | 79.9 | 20.1 |
| Thin oxide Mk16B | 46.1 | 0.5 | 51.2 | 2.2 | | 0.1 | | 47.4 | 52.6 |
| USH | 63.4 | 0.1 | 35.7 | 0.7 | 0.1 | 0.1 | 0.1 | 64.0 | 36.0 |
| MURR | 77.6 | 0.0 | 22.3 | | | 0.1 | | 77.7 | 22.3 |

The USH EDS results suggest a predominantly boehmite film, the EDS probe picking up signal from the underlying alloy, or a combination of the two. The EDS results for the thick Mark-16B and the MURR both appear to indicate bayerite and/or gibbsite. The cross-section SEM indicated both films are thicker than the estimated spatial resolution of the EDS, so signal from the underlying material is unlikely to play a role. The thin oxide Mark-16B results indicate a lower oxygen content than any expected aluminum oxide, most likely reflecting a contribution from aluminum substrate beneath the thin film.

DISCUSSION

Composition (XRD)

Bayerite and boehmite were found on all three samples, but gibbsite was found on only the Mark-16B. Trihydroxides (bayerite and gibbsite) form at temperatures below ~80°C.[24] Based on the comparison of the (oxy)hydroxide XRD peaks, known operation histories, length of time in wet storage, and assuming the (oxy)hydroxide layer formation was not dominated by growth in the wet storage pool, it can be inferred that the USH was exposed to the highest (boehmite-forming) temperatures, followed by the MURR, and the Mark-16B having the lowest temperature exposure. The presence of bayerite on the USH, which is believed to have operated close to 90°C and thus expected to form boehmite in-core, suggests that further oxide growth in wet storage may be significant even in the presence of an existing boehmite film.

The extent to which the presence of boehmite impacts the growth of gibbsite and bayerite is unknown and may complicate the growth and relative ratios of (oxy)hydroxides. Characterization of surrogate (oxy)hydroxide films grown without pre-existing boehmite on Al-1100 using a hot-wall immersion method at 50 °C [25] identified the oxide as bayerite, a trihydroxide polymorph. Films grown on Al-6061 under similar conditions [26] were also identified as predominantly bayerite, possibly accompanied by a smaller amount of gibbsite. The specific trihydroxide polymorphs formed for corrosion below ~80 °C have been found to depend on environmental characteristics such as pH and/or presence of impurities in the water, with bayerite formation associated with the absence of impurities and near-neutral pH (~5.8 to ~9) while gibbsite was associated with the presence of impurities (such as solutions of NaOH or KOH) or high (>9) or low (<5.8) pH [14, 24].

Morphology

Thick, blocky bayerite films grown in the lab [23, 27] displayed a multilayered structure in cross-section. This layered structure is consistent with literature descriptions of sequential formation of pseudoboehmite followed by trihydroxide growth on top of the existing pseudoboehmite layer [28]. By contrast, the

(oxy)hydroxide films in the present study that were identifiable in cross-section (MURR and Mark-16B, Fig. 11) do not appear to have more than one visible layer.

The reason for this difference in structure is not immediately clear. One significant difference between the lab-grown and service-formed (oxy)hydroxide layers is time: the lab-grown samples were grown in weeks to months, while the samples characterized in the present study have been immersed in water for decades. It is possible that the (oxy)hydroxide films have continued to evolve over this long storage duration, converting initially distinct layers of (oxy)hydroxide into a uniform film. In addition, the service-formed (oxy)hydroxides were constantly exposed to radiation while the lab-grown surrogates were grown in an unirradiated environment, which could also have impacted the structure of the film.

CONCLUSIONS

(Oxy)hydroxides on the cladding of three service-exposed Al-6061 and Al-6063 croppings were characterized after wet storage for up to 50 years in L-Basin on the Savannah River Site. SEM, EDS, and XRD were performed on samples to evaluate the composition and morphology of the (oxy)hydroxide films. (Oxy)hydroxides on the cladding of all three croppings were identified by XRD and confirmed by EDS. XRD revealed bayerite ($\text{Al}(\text{OH})_3$) and boehmite (AlOOH) on the MURR and USH samples and bayerite, boehmite, and gibbsite ($\text{Al}(\text{OH})_3$) on the Mark-16B sample. Comparison of relative peak intensities suggests that the USH had the most boehmite, followed by the MURR, and finally the Mark-16B. This is consistent with the operating temperatures estimated from available information on the material histories. The surface morphologies were blocky for all three films.

Predicted and characterized values of (oxy)hydroxide layer thickness are compared in TABLE IV.

TABLE IV. Oxide thickness summary and comparison to values estimated from literature.

| Sample | Estimated range* (μm) | Observed range (μm) |
|----------|------------------------------------|----------------------------------|
| MURR | 4-5 | 5-10 |
| USH | 2-16 | Not detected |
| Mark-16B | 0-14 | 5-15 |

REFERENCES

- [1] R. Butler, et al., "Missouri University Research Reactor (MURR) Safety Analysis Report," University of Missouri, Columbia MU Project # 000763, August 18 2006.
- [2] J. Stillman, E. Feldman, L. Foyto, K. Kutikkad, J. C. McKibben, N. Peters, *et al.*, "Technical Basis in Support of the Conversion of the University of Missouri Research Reactor (MURR) Core from Highly-Enriched to Low-Enriched Uranium – Core Neutron Physics," Argonne National Laboratory ANL/RERTR/TM-12-30, September 2012.
- [3] J. Stillman, E. Feldman, L. Foyto, K. Kutikkad, J. C. McKibben, N. Peters, *et al.*, "Conceptual Design Parameters for MURR LEU U-Mo Fuel Conversion Design Demonstration Experiment," Argonne National Laboratory ANL/RERTR/TM-12-38, Rev. 1, March 2013.
- [4] L. Foyto, "RE: Fuel storage pool pH and pool water chemistry," L. Olson, Ed., MURR Pool Water Chemistry data/trends for calendar year 2018 ed. SRNL, 2019.
- [5] J. P. Howell, P. E. Zapp, and D. Z. Nelson, "Corrosion of aluminum alloys in a reactor disassembly basin," Westinghouse Savannah River Company WSRC-MS-92-393, 1992.
- [6] K. E. Metzger, "Task Technical and Quality Assurance Plan for Aluminum Clad SNF Dry Storage Studies," Savannah River National Laboratory SRNL-RP-2018-00610, June 6 2018.
- [7] D. Rose, "FW: USH and Mark-16B steam drying temperature and time," C. Verst, Ed., ed, Feb. 6, 2019.

- [8] Savannah River Site, "Table 5.4-1 Process Water System Heat Exchanger Design Data," SRS Production Reactor SAR, Ed., ed, 1989, p. 0506/E/1.
- [9] M. Dunsmuir, "MK 16B and USH history," K. Metzger and C. Verst, Eds., ed. SRNL, May 9, 2018.
- [10] Savannah River Plant, "Auxiliary Sleeve ('B' Outer Chuck), Savannah River Plant technical drawing," ST-MDX58835, Ed., ed, 1974.
- [11] Savannah River Plant, "Mark-16B Assembly (U), Savannah River Plant technical drawing," ST-MDX5-9147, Ed., ed, 1976.
- [12] J. P. Howell, "Corrosion Surveillance In Spent Fuel Storage Pools," presented at the Corrosion97, New Orleans, Louisiana, 1997.
- [13] L. Olson, C. Verst, A. d'Entremont, R. Fuentes, and R. Sindelar, "Characterization of Oxide Films on Aluminum Materials following Reactor Exposure and Wet Storage in the SRS L-Basin," Savannah River National Laboratory SRNL-STI-2019-00058, 2019.
- [14] K. Wefers and C. Misra, "Oxides and hydroxides of aluminum," Alcoa Laboratories Pittsburgh, PA Alcoa Technical Paper #19, 1987.
- [15] J. E. Draley, S. Mori, and R. E. Loess, "The Corrosion of 1100 Aluminum in Oxygen-Saturated Water at 70°C," *Journal of The Electrochemical Society*, vol. 110, pp. 622-627, 1963.
- [16] J. E. Draley, S. Mori, and R. E. Loess, "The Corrosion of 1100 Aluminum in Water from 50° to 95° C," *Journal of The Electrochemical Society*, vol. 114, pp. 353-354, 1967.
- [17] S. J. Pawel, D. K. Felde, and R. E. Pawel, "Influence of coolant pH on corrosion of 6061 aluminum under reactor heat transfer conditions," Oak Ridge National Laboratory 1995.
- [18] P. D. Neumann, "Corrosion in the Oak Ridge Research Reactor Core-Cooling system," Oak Ridge National Laboratory 1960.
- [19] P. D. Neumann, "The corrosion of aluminum alloys in the Oak Ridge Research Reactor," Oak Ridge National Laboratory 1961.
- [20] M. Dewar, "Characterization and Evaluation of Aged 20Cr32Ni1Nb Stainless Steels," Master of Science in Materials Engineering, Department of Chemical and Materials Engineering, University of Alberta, Edmonton, Alberta, 2013.
- [21] J. Goldstein, D. E. Newbury, D. C. Joy, C. E. Lyman, P. Echlin, E. Lifshin, *et al.*, *Scanning Electron Microscopy and X-Ray Microanalysis*, 3 ed.
- [22] L. Olson, R. Fuentes, A. d'Entremont, and R. Sindelar, "Characterization of Oxyhydroxides on a Dry-Stored Fuel Plate From L-Basin," SRNL-STI-2018-00428, October 2018.
- [23] A. L. d'Entremont, R. E. Fuentes, M. G. Shalloo, T. W. Knight, and R. L. Sindelar, "Thermal Dehydration of Aluminum (Oxy)hydroxides on Fuel Cladding Material " presented at the Waste Management Symposia 2020, Phoenix, AZ, 2020.
- [24] B. Rabin, M. Meyer, J. Cole, I. Glagolenko, G. Hofman, W. Jones, *et al.*, "Preliminary Report on U-Mo Monolithic Fuel for Research Reactors," Idaho National Laboratory INL/EXT-17-40975, 2017.
- [25] K. E. Metzger, R. Fuentes, A. d'Entremont, L. Olson, and R. Sindelar, "Preparation of aluminum oxide films under water exposure - Preliminary report on 1100 series alloys," Savannah River National Laboratory SRNL-STI-2018-00427, 2018.
- [26] A. L. d'Entremont, R. E. Fuentes, L. C. Olson, and R. L. Sindelar, "Preparation of Aluminum Oxide Films Under Water Exposure – Preliminary Report on 6061 Series Alloys," Savannah River National Laboratory SRNL-STI-2018-00449, 2018.
- [27] A. L. d'Entremont, R. E. Fuentes, L. C. Olson, and R. L. Sindelar, "Preparation of Aluminum Oxide Films Under Water Exposure – Preliminary Report on 5052 Series Alloys," Savannah River National Laboratory SRNL-STI-2018-00646, 2018.
- [28] R. K. Hart, "The formation of films on aluminium immersed in water," *Transactions of the Faraday Society*, vol. 53, pp. 1020-1027, 1957.